Author Manuscript

Author Manuscript

Author Manuscript

Author Manuscript

HHS Public Access

Author manuscript

Nature. Author manuscript; available in PMC 2020 November 12.

Published in final edited form as:

Nature. 2020 September ; 585(7824): 268–272. doi:10.1038/s41586-020-2324-7.

Respiratory disease in rhesus macaques inoculated with SARS-CoV-2

Vincent J. Munster[1], **Friederike Feldmann**[2], **Brandi N. Williamson**[1], **Neeltje van Doremalen**[1], **Lizzette Pérez-Pérez**[1], **Jonathan Schulz**[1], **Kimberly Meade-White**[1], **Atsushi Okumura**[1], **Julie Callison**[1], **Beniah Brumbaugh**[3], **Victoria A. Avanzato**[1], **Rebecca Rosenke**[2], **Patrick W. Hanley**[2], **Greg Saturday**[2], **Dana Scott**[2], **Elizabeth R. Fischer**[3], **Emmie de Wit**[1,*]

[1]Laboratory of Virology, National Institute of Allergy and Infectious Diseases, National Institutes of Health, Hamilton, MT, United States of America

[2]Rocky Mountain Veterinary Branch, National Institute of Allergy and Infectious Diseases, National Institutes of Health, Hamilton, MT, United States of America

[3]Research Technologies Branch, National Institute of Allergy and Infectious Diseases, National Institutes of Health, Hamilton, MT, United States of America

Abstract

An outbreak of a novel coronavirus, named SARS-CoV-2, causing respiratory disease and a ~2% case fatality rate started in Wuhan, China in December 2019[1,2]. Following unprecedented global spread3, the World Health Organization declared COVID-19 a pandemic on March 11, 2020. Although data on disease in humans are emerging at a steady pace, certain aspects of the pathogenesis of SARS-CoV-2 can only be studied in detail in animal models, where repeated sampling and tissue collection is possible. Here, we show that SARS-CoV-2 causes respiratory disease in infected rhesus macaques, with disease lasting 8–16 days. Pulmonary infiltrates, a hallmark of human disease, were visible in lung radiographs. High viral loads were detected in swabs from the nose and throat of all animals as well as in bronchoalveolar lavages; in one animal we observed prolonged rectal shedding. Taken together, the rhesus macaque recapitulates moderate disease observed in the majority of human cases. The establishment of the rhesus macaque as a model of COVID-19 will increase our understanding of the pathogenesis of this disease and will aid development and testing of medical countermeasures.

SARS-CoV-2 infection in humans can be asymptomatic or result in mild to fatal Coronavirus Disease 2019 (COVID-19)[4–6]. Patients with COVID-19 pneumonia presented mainly with fever, fatigue, dyspnea and cough[7–9]. Rapidly progressing pneumonia, with bilateral opacities on x-ray or patchy shadows and ground glass opacities by CT scan were

---

Users may view, print, copy, and download text and data-mine the content in such documents, for the purposes of academic research, subject always to the full Conditions of use:http://www.nature.com/authors/editorial_policies/license.html#terms

*Corresponding author: Emmie.dewit@nih.gov.

Author contributions

VJM and EdW designed the study; VJM, FF,BW, NvD, LPP, JS, KMW, AO, JC, BB, VAA, RR, PH, GS, EF, DS and EdW acquired, analyzed and interpreted the data; VJM, PH, EF, DS and EdW wrote the manuscript. All authors have approved the submitted version.

Competing interests

The authors declare no competing interests

Author Manuscript Author Manuscript Author Manuscript Author Manuscript

observed in COVID-19 patients[2,6,10]. Older patients with comorbidities are at highest risk for adverse outcome of COVID-19[5,7]. SARS-CoV-2 has been detected in upper and lower respiratory tract samples from patients, as well as feces and blood, but not in urine[5,11–13].

Non-human primate models that recapitulate aspects of human disease are essential for our understanding of the pathogenic processes involved in severe respiratory disease and the development of medical countermeasures such as vaccines and antivirals.

Clinical, respiratory disease

Eight adult rhesus macaques were inoculated with SARS-CoV-2 isolate nCoV-WA1–2020[14]. On day 1 post inoculation (dpi), all animals showed changes in respiratory pattern and piloerection, as reflected in their clinical scores (Fig. 1a). Other observed signs of disease included reduced appetite, hunched posture, pale appearance and dehydration (Extended Data Table 1). Coughing was occasionally heard in the room where animals were housed but could not be pinpointed to individual animals. Disease signs persisted for more than a week, with all animals completely recovered between 9 and 17 dpi (Fig. 1a and Table S1). Weight loss was observed in all animals (Fig. 1b); body temperatures spiked on 1 dpi but returned to normal levels thereafter (Fig. 1c). Under anesthesia, the animals did not show increased respiration; however, all animals showed irregular respiration patterns (Fig. 1d). Radiographs showed pulmonary infiltrates in all animals starting on 1 dpi with mild pulmonary infiltration primarily in the lower lung lobes. By 3 dpi, progression of mild pulmonary infiltration was noted into other lung lobes although still primarily in the caudal lung lobes (Fig. 1e). In one animal, pulmonary infiltrates were observed from 1–12 dpi (Extended Data Fig. 1).

Hematologic analysis of blood collected during clinical exams showed evidence of a stress leukogram[15] by 1 dpi in the majority of animals (Extended Data Fig. 2). Lymphocytes and monocytes returned to baseline after 1 dpi. Neutrophils decreased in all animals by 3 dpi and continued to decline through 5 dpi; neutropenia was observed in 2 of 4 animals. On 1 dpi, decreased hematocrit, red blood cell counts and hemoglobin were observed in all animals (Extended Data Fig. 2). In addition, reticulocyte percentages and counts decreased. At 5 dpi, two of four animals had a normocytic, normochromic non-regenerative anemia consistent with anemia of critical illness; animals did not return to their original baselines by 21 dpi. Blood chemistry analysis revealed no values outside normal range (Supplementary Information Table S2).

Serum was analyzed for changes in cytokine and chemokine levels at different time points after inoculation. Statistically significant changes were only observed on 1 dpi, with increases in IL1ra, IL6, IL10, IL15, MCP-1, MIP-1b, and on 3 dpi a small but statistically significant decrease in TGFα was observed (Extended Data Fig. 3). Although changes occurred in the levels of some of these cytokines later after inoculation, these were not statistically significant (Extended Data Fig. 3).

Author Manuscript Author Manuscript Author Manuscript Author Manuscript

High viral loads in respiratory samples

Virus shedding was highest from the nose (Fig. 2a); virus could be isolated from swabs collected on 1 and 3 dpi, but not thereafter. Viral loads were high in throat swabs immediately after inoculation but were less consistent than nose swabs thereafter; in one animal throat swabs were positive on 1 and 10 dpi but not in between (Fig. 2a). One animal showed prolonged shedding of viral RNA in rectal swabs; infectious virus could not be isolated from these swabs (Fig. 2a) and intestinal tract disease (e.g. diarrhea) was not observed. Urogenital swabs remained negative in all animals throughout the study. On 1, 3 and 5 dpi bronchoalveolar lavages (BAL) were performed on the 4 animals in the group euthanized on 21 dpi. High viral loads were detected in BAL fluid in all animals on all three time points; infectious virus could only be isolated in BAL fluid collected on 1 and 3 dpi (Fig. 2b). No viral RNA could be detected in blood (Fig. 2c) or urine (Fig. 2d).

Interstitial pneumonia

On 3 and 21 dpi, one group of 4 animals was euthanized and necropsies were performed. On 3 dpi, varying degrees of gross lung lesions were observed in all animals (Fig. 3a and c). By 21 dpi, gross lesions were still visible in the lungs of 2 of 4 animals (Fig. 3b and c). Additionally, all animals had an increased lung weight:body weight ratio (Fig. 3d) as compared to healthy rhesus macaques, indicative of pulmonary edema. Histologically, 3 of the 4 animals euthanized on 3 dpi developed some degree of pulmonary pathology. Lesions were multifocal (Extended Data Fig. 4a), mild to moderate, interstitial pneumonia that frequently centered on terminal bronchioles. The pneumonia was characterized by thickening of alveolar septae by edema fluid and fibrin and small to moderate numbers of macrophages and fewer neutrophils. Lungs with moderate changes also had alveolar edema and fibrin with formation of hyaline membranes. There was minimal type II pneumocyte hyperplasia. Occasionally, bronchioles showed necrosis, loss and attenuation of the epithelium with infiltrates of neutrophils, macrophages and eosinophils. Multifocally, there were perivascular infiltrates of small numbers of lymphocytes forming perivascular cuffs (Extended Data Figure 4b) and minimal to mild, multifocal hyperplasia of bronchiolar associated lymphoid tissue. Three of 4 animals on 3 dpi had fibrous adhesions of the lung to the pleura. Histologic evaluation showed these to be composed of mature collagen interspersed with small blood vessels; therefore, this is most likely a chronic change rather than related to SARS-CoV-2 infection. Minimal to mild inflammation was observed in the upper airways with multifocal squamous metaplasia of the respiratory epithelium with infiltration of small numbers of neutrophils (Extended Data Figure 5).

Immunohistochemistry using a mAb against SARS-CoV demonstrated viral antigen in small numbers of type I and II pneumocytes, as well as alveolar macrophages. Antigen-positive macrophages were detected in mediastinal lymph nodes of 3 of 4 animals (Fig. 3k). Interestingly, small numbers of antigen-positive lymphocytes and macrophages were also detected in the lamina propria of the intestinal tract of all 4 animals. In one animal, all collected tissues of the gastrointestinal tract showed these antigen-positive mononuclear cells (Extended Data Figure 6).

Author Manuscript Author Manuscript Author Manuscript Author Manuscript

Ultrastructural analysis of lung tissue by transmission electron microscopy confirmed the histologic diagnosis of interstitial pneumonia. The alveolar interstitial space was greatly expanded by edema, fibrin, macrophages and neutrophils (Extended Data Figure 7a). The subepithelial basement membrane was unaffected and maintained a consistent thickness and electron density. Occasionally, type I pneumocytes are separated from the basement membrane by edema; the resulting space may contain virions. Affected type I pneumocytes are lined by small to moderate numbers of virions 90–160 nm in diameter with an electron dense core bound by a less dense capsid (Extended Data Figure 7b–e). Alveolar spaces adjacent to affected pneumocytes are filled with a granular, moderately electron dense material that is consistent with edema fluid.

Replication in the respiratory tract

All tissues (n=37) collected at necropsy were analyzed for the presence of viral RNA. On 3 dpi, high viral loads were detected in the lungs of all animals (Extended Data Fig. 8a); virus could be isolated from the lungs of all 4 animals at this time. Additionally, viral RNA could be detected in other samples throughout the respiratory tract (Extended Data Fig. 8), as well as in lymphoid and gastrointestinal tissues. Viral RNA could not be detected in major organs including the central nervous system. To distinguish viral RNA derived from respiratory secretions from active virus replication, all samples with presence of viral RNA were also tested for the presence of viral mRNA (Extended Data Fig. 8). Viral mRNA was detected in all respiratory tissues but could not in any but one of the gastrointestinal tissues, indicating that virus replication in these tissues seems unlikely, although we can’t exclude it due to limited sample size. By 21 dpi, viral RNA, but not mRNA, could still be detected in tissues from all 4 animals (Extended Data Fig. 8g).

Serology

Serum was analyzed for the development of IgG against SARS-CoV spike in ELISA. By 10 dpi, all four animals had seroconverted to SARS-CoV-2 spike; neutralizing responses also started to appear at 10 dpi (Extended Data Figure 9). Interestingly, the animal with the lowest and latest neutralizing antibody response was the animal with prolonged viral shedding from the intestinal tract.

Discussion

COVID-19 clinical manifestations range from asymptomatic to mild to severe[5,6,8,9,13,16]. Patients present with influenza-like symptoms such as fever and shortness of breath and may develop pneumonia requiring mechanical ventilation and support in an intensive care unit[9]. Similar to SARS-CoV and MERS-CoV, comorbidities such as hypertension and diabetes play an important role in adverse outcome of COVID-19[8,17,18]. Advanced age and chronic conditions in particular are indicators of a negative outcome[5,7–9,16], conditions that were absent in our healthy rhesus macaques. An analysis of 1099 COVID-19 cases from China showed that approximately 5% of diagnosed patients developed severe pneumonia requiring ICU attendance, 2.3% required mechanical ventilation and 1.4% died[9]. The transient, moderate disease observed here in rhesus macaques is thus in line with the majority of

Author Manuscript Author Manuscript Author Manuscript Author Manuscript

human COVID-19 cases. Pulmonary infiltrates on radiographs, a hallmark of human infection[2,4,6,7,9,10,16], were observed in all macaques. The shedding pattern observed in rhesus macaques is strikingly similar to that observed in humans[11,12]. In humans, consistent high SARS-CoV-2 shedding was observed from the upper and lower respiratory tract, frequent intermediate shedding from the intestinal tract and sporadic detection in blood[5]. Similar to humans, shedding of SARS-CoV-2 continued after resolution of clinical symptoms and radiologic abnormalities [19]. Limited histopathology is available from COVID-19 patients[20,21]. Our analysis of the histopathological changes observed in the lungs of rhesus macaques, suggests that they resemble those observed with SARS-CoV and MERS-CoV [21–24], with regard to lesion type and cell tropism.

Serological responses in humans are not typically detectable before 6 days after symptom onset, with IgG titers between 100 and 10,000 observed after 12 to 21 days[25,26]. Neutralizing titers were generally between 20 – 160. This corresponds to the results in our rhesus macaque model, where IgG responses were detected around 7–10 dpi. Seroconversion was not directly followed by a decline in viral loads, as observed in COVID-19 patients[25,26].

Taken together, the rhesus macaque model recapitulates COVID-19, with regard to virus replication and shedding, the presence of pulmonary infiltrates, histological lesions and seroconversion. This extensive dataset allows us to bridge between the rhesus macaques model and the disease observed in humans and to utilize this animal model to assess the efficacy of medical countermeasures.

Methods

Ethics and biosafety statement

All animal experiments were approved by the Institutional Animal Care and Use Committee of Rocky Mountain Laboratories, NIH and carried out by certified staff in an Association for Assessment and Accreditation of Laboratory Animal Care (AAALAC) International accredited facility, according to the institution’s guidelines for animal use, following the guidelines and basic principles in the NIH Guide for the Care and Use of Laboratory Animals, the Animal Welfare Act, United States Department of Agriculture and the United States Public Health Service Policy on Humane Care and Use of Laboratory Animals. Rhesus macaques were housed in adjacent individual primate cages allowing social interactions, in a climate-controlled room with a fixed light-dark cycle (12-hr light/12-hr dark). Animals were monitored at least twice daily throughout the experiment. Commercial monkey chow, treats, and fruit were provided twice daily by trained personnel. Water was available ad libitum. Environmental enrichment consisted of a variety of human interaction, manipulanda, commercial toys, videos, and music. The Institutional Biosafety Committee (IBC) approved work with infectious SARS-CoV-2 strains under BSL3 conditions. Sample inactivation was performed according to IBC-approved standard operating procedures for removal of specimens from high containment.

Author Manuscript Author Manuscript Author Manuscript Author Manuscript

Study design

To evaluate the use of rhesus macaques as a model for SARS-CoV-2, eight adult rhesus macaques (4 males, and4 females, age 4–6 years) were inoculated via a combination of intranasal (0.5ml per nostril), intratracheal (4ml), oral (1ml) and ocular (0.25ml per eye) of a 4×10^5 TCID50/ml (3×10^8 genome copies/ml) virus dilution in sterile DMEM. The animals were observed twice daily for clinical signs of disease using a standardized scoring sheet (Supplementary Information Table S1); the same person assessed the animals throughout the study. The predetermined endpoint for this experiment was 3 days post inoculation (dpi) for one group of 4 animals, and 21 dpi for the remaining 4 animals. Animals were randomly assigned to a group for necropsy prior to the start of the experiment. Blinding was not used in this study since all animals were subjected to the same treatment. Clinical exams were performed on 0, 1, 3, 5, 7, 10, 12, 14, 17 and 21 dpi on anaesthetized animals. On exam days, clinical parameters such as bodyweight, body temperature and respiration rate were collected, as well as ventro-dorsal and lateral chest radiographs. Chest radiographs were interpreted by a board-certified clinical veterinarian. The following samples were collected at all clinical exams: nasal, throat, urogenital and rectal swabs, blood. The total white blood cell count, lymphocyte, neutrophil, platelet, reticulocyte and red blood cell counts, hemoglobin, and hematocrit values were determined from EDTA blood with the IDEXX ProCyte DX analyzer (IDEXX Laboratories). Serum biochemistry (albumin, AST, ALT, GGT, BUN, creatinine) was analyzed using the Piccolo Xpress Chemistry Analyzer and Piccolo General Chemistry 13 Panel discs (Abaxis). During clinical exams on 1, 3, and 5 dpi bronchoalveolar lavages were performed using 10ml sterile saline. Of note, repeated bronchoalveolar lavages do not induce lung damage when space 48 hrs apart[27,28]. After euthanasia, necropsies were performed. The percentage of gross lung lesions was scored by a board-certified veterinary pathologist and samples of the following tissues were collected: inguinal lymph node, axillary lymph node, cervical lymph node, salivary gland, conjunctiva, nasal mucosa, oropharynx, tonsil, trachea, all six lung lobes, mediastinal lymph node, right and left bronchus, heart, liver, spleen, pancreas, adrenal gland, kidney, mesenteric lymph node, stomach, duodenum, jejunum, ileum, cecum, colon, urinary bladder, reproductive tract (testes or ovaries depending on sex of the animal), bone marrow, frontal brain, cerebellum and brainstem. Histopathological analysis of tissue slides was performed by a board-certified veterinary pathologist blinded to the group assignment of the animals.

Virus and cells

SARS-CoV-2 isolate nCoV-WA1–2020 (MN985325.1)[14] (Vero passage 3) was kindly provided by CDC and propagated once in VeroE6 cells in DMEM (Sigma) supplemented with 2% fetal bovine serum (Gibco), 1 mM L-glutamine (Gibco), 50 U/ml penicillin and 50 μg/ml streptomycin (Gibco) (virus isolation medium). The used virus stock was 100% identical to the initial deposited genbank sequence (MN985325.1) and no contaminants were detected. VeroE6 cells were maintained in DMEM supplemented with 10% fetal calf serum, 1 mM L-glutamine, 50 U/ml penicillin and 50 μg/ml streptomycin. VeroE6 cells were provided by Dr. Ralph Baric and were not authenticated in-house; mycoplasma testing is performed at regular intervals and no mycoplasma has been detected.

Author Manuscript Author Manuscript Author Manuscript Author Manuscript

Quantitative PCR

RNA was extracted from swabs and BAL using the QiaAmp Viral RNA kit (Qiagen) according to the manufacturer's instructions. Tissues (30 mg) were homogenized in RLT buffer and RNA was extracted using the RNeasy kit (Qiagen) according to the manufacturer's instructions. For detection of viral RNA, 5 μl RNA was used in a one-step real-time RT-PCR E assay[29] using the Rotor-Gene probe kit (Qiagen) according to instructions of the manufacturer. In each run, standard dilutions of counted RNA standards were run in parallel, to calculate copy numbers in the samples. For detection of SARS-CoV-2 mRNA, primers targeting open reading frame 7 (ORF7) were designed as follows: forward primer 5'-TCCCAGGTAACAAACCAACC-3', reverse primer 5'-GCTCACAAGTAGCGAGTGTTAT-3', and probe FAM-ZEN-CTTGTAGATCTGTTCTCTAAACGAAC-IBFQ. 5 μl RNA was used in a one-step real-time RT-PCR using the Rotor-Gene probe kit (Qiagen) according to instructions of the manufacturer. In each run, standard dilutions of counted RNA standards were run in parallel, to calculate copy numbers in the samples.

Histopathology and immunohistochemistry

Histopathology and immunohistochemistry were performed on rhesus macaque tissues. After fixation for a minimum of 7 days in 10 % neutral-buffered formalin and embedding in paraffin, tissue sections were stained with hematoxylin and eosin (HE). To detect SARS-CoV-2 antigen, immunohistochemistry was performed using an anti-SARS nucleocapsid protein antibody (Novus Biologicals) at a 1:250 dilution. This antibody was first tested on SARS-CoV-2 infected and uninfected Vero E6 cell pellets, showing specific staining with infected cells and no staining with uninfected cells. The antibody showed specific staining with infected experimental tissue and no staining with uninfected tissue from rhesus macaques. Infected tissue and cell pellet specimens showed no staining when run with Rabbit IgG controls (non-specific rabbit IgG substituted for primary antibody). Stained slides were analyzed by a board-certified veterinary pathologist.

Transmission electron microscopy—After fixation for 7 days with Karnovsky's fixative at 4° C, excised tissues were post-fixed for 1 hour with 0.5% osmium tetroxide/0.8% potassium ferricyanide in 0.1 M sodium cacodylate, washed 3 × 5 minutes with 0.1M sodium cacodylate buffer, stained 1 hour with 1% tannic acid, washed with buffer and then further stained with2% osmium tetroxide in 0.1M sodium cacodylate and overnight with 1% uranyl acetate at 4° C. Specimens were dehydrated with a graded ethanol series with two final exchanges in 100% propylene oxide before infiltration and final embedding in Embed-812/Araldite resin. Thin sections were cut with a Leica EM UC6 ultramicrotome (Leica, Vienna, Austria), prior to viewing at 120 kV on a Tecnai BT Spirit transmission electron microscope (Thermo fisher/FEI, Hillsboro, OR). Digital images were acquired with a Gatan Rio bottom mount digital camera system (Gatan Inc., Pleasanton, CA and processed using Adobe Photoshop v. CC 2019 (Adobe Systems Inc, San Jose, CA).

Serum cytokine and chemokine analysis—Serum samples for analysis of cytokine/chemokine levels were inactivated with γ-radiation (2 MRad) according to standard operating procedures. Concentrations of granulocyte colony-stimulating factor, granulocyte-

Author Manuscript Author Manuscript Author Manuscript Author Manuscript

macrophage colony-stimulating factor, interferon (IFN)–γ, interleukin (IL)–1β, IL-1 receptor antagonist, IL-2, IL-4, IL-5, IL-6, IL-8, IL-10, IL-12/23 (p40), IL-13, IL-15, IL-17, MCP-1 and macrophage inflammatory protein (MIP)–1α, MIP-1β, soluble CD40-ligand (sCD40L), transforming growth factor-α, tumor necrosis factor (TNF)–α, vascular endothelial growth factor (VEGF) and IL-18 were measured on a Bio-Plex 200 instrument (Bio-Rad) using the Non-Human Primate Cytokine MILLIPLEX map 23-plex kit (Millipore) according to the manufacturer's instructions.

Serology

Sera were analyzed by SARS-CoV-2 spike protein (S) enzyme-linked immunosorbent assay (ELISA) as done previously for MERS-CoV[30]. Briefly, maxisorp (Nunc) plates were coated overnight with 100 ng/well S protein diluted in PBS[31] (a kind gift of Barney Graham, Vaccine Research Center, NIH) and blocked with blocker casein in PBS (Life Technologies). Sera were serially diluted in duplicate. SARS-CoV-2-specific antibodies were detected using anti-monkey IgG polyclonal antibody HRP-conjugated antibody (KPL), peroxidase-substrate reagent (KPL) and stop reagent (KPL). Optical density (OD) was measured at 405 nm. The threshold of positivity was calculated by taking the average of the day 0 values multiplied by 3.

For neutralization, sera were heat-inactivated (30 min, 56 °C) and two-fold serial dilutions were prepared in 2% DMEM. Hereafter, 100 $TCID_{50}$ of SARS-CoV-2 was added. After 60 min incubation at 37 °C, virus:serum mixture was added to VeroE6 cells and incubated at 37°C and 5% CO2. At 5 dpi, cytopathic effect was scored. The virus neutralization titer is expressed as the reciprocal value of the highest dilution of the serum which still inhibited virus replication. All sera were analyzed in duplicate.

Data availability

Data have been deposited in Figshare: https://doi.org/10.35092/yhjc.12026910.

Author Manuscript
Author Manuscript
Author Manuscript
Author Manuscript

Extended Data

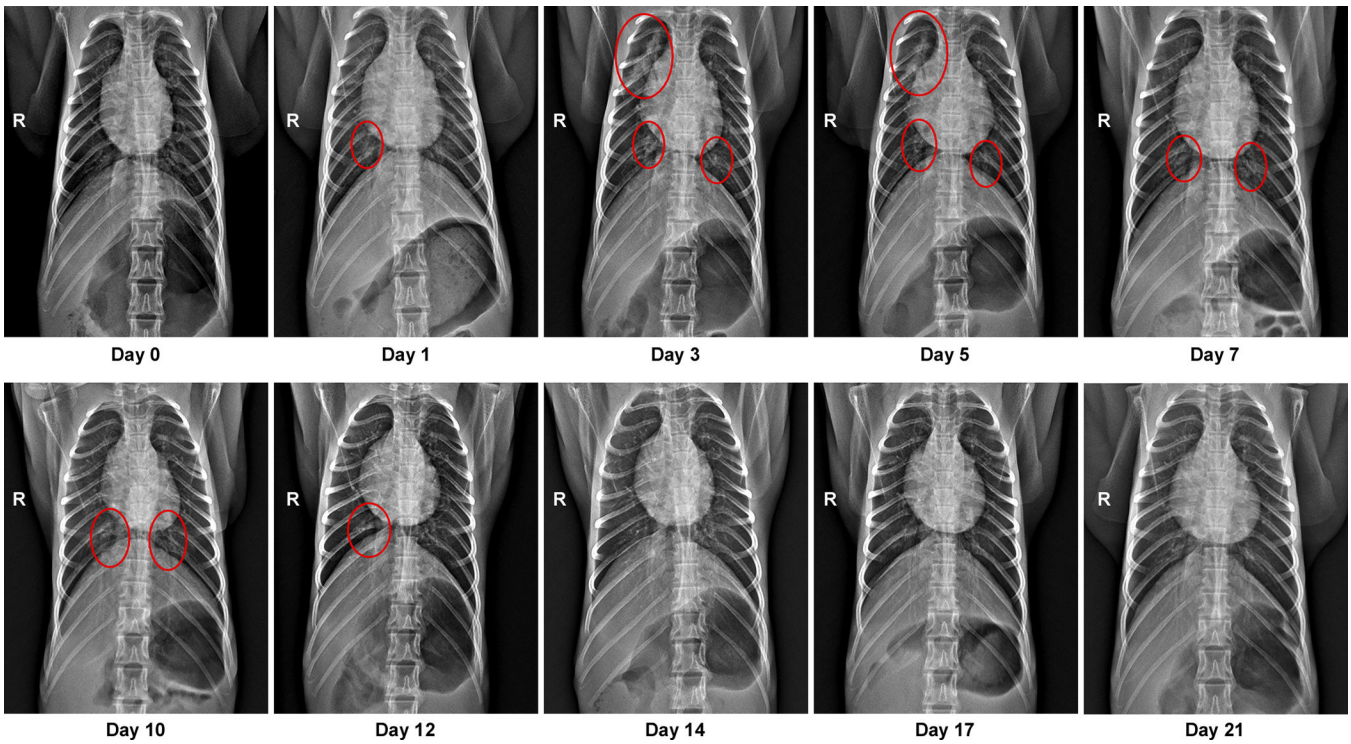

Extended Data Figure 1. Pulmonary infiltrates in a rhesus macaque after inoculation.
Radiographs show the progression of pulmonary infiltrates throughout the study in a single animal. Of note, this animal is denoted with a black triangle throughout the manuscript. Circles indicate areas of mild to moderate pulmonary infiltrates. A marker 'R' indicates right side of the animal. Three chest radiographs were taken at each timepoint: right-lateral, left-lateral and ventro-dorsal; only the ventro-dorsal radiograph is shown.

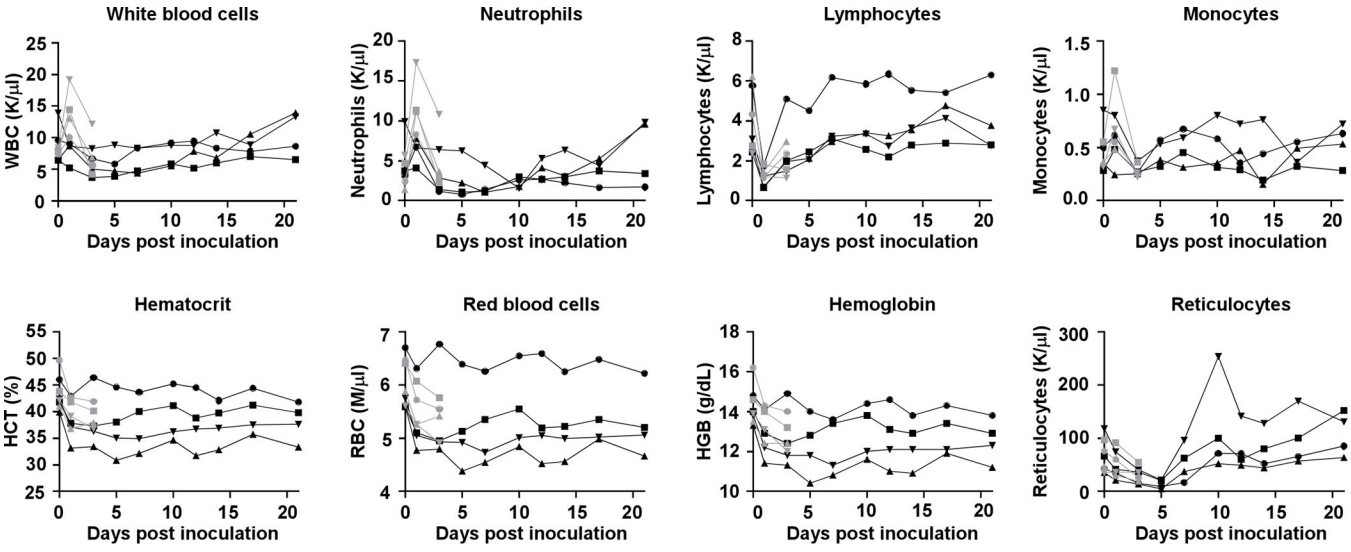

Extended Data Figure 2. Hematological changes in rhesus macaques infected with SARS-CoV-2.

Author Manuscript
Author Manuscript
Author Manuscript
Author Manuscript

Identical symbols have been used to denote identical animals throughout the figures in this manuscript. n= 8 animals on 0, 1, and 3 dpi and n=4 animals thereafter.

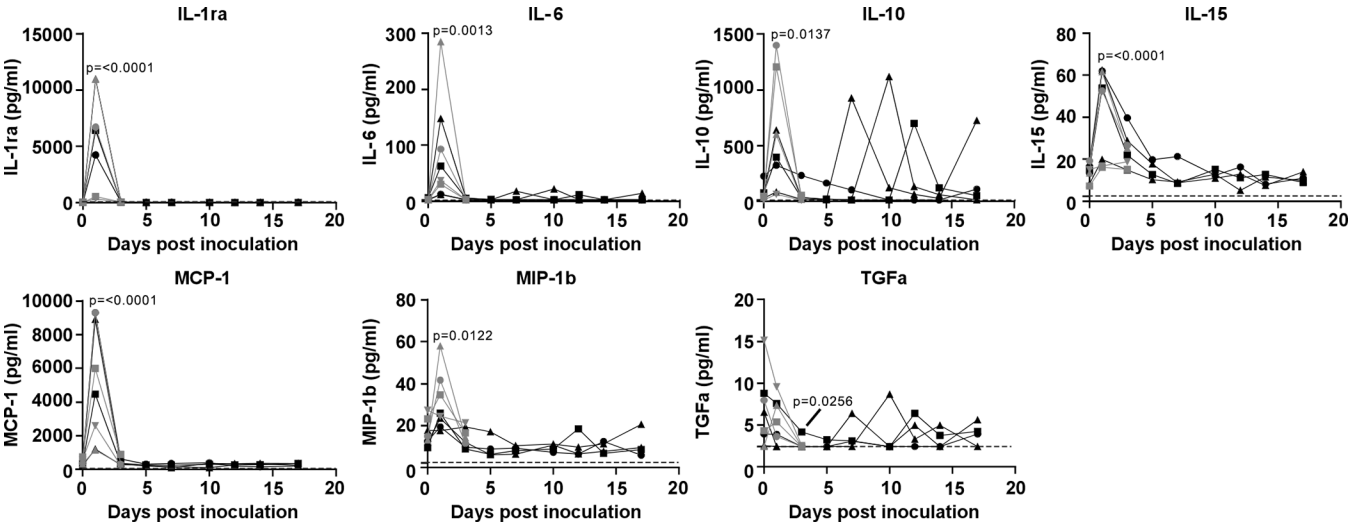

Extended Data Figure 3. Cytokine and chemokine levels in serum of rhesus macaques infected with SARS-CoV-2.

The levels of 23 cytokines and chemokines were determined in serum at different timepoints after inoculation. Levels are displayed only for those cytokines and chemokines where statistically significant (1-way ANOVA) were observed compared to levels on day of inoculation. Identical symbols have been used to denote identical animals throughout the figures in this manuscript. The lower limit of detection is indicated with a dotted line. Serum samples were analyzed in duplicate from each animal for each timepoint; n= 8 animals on 0, 1, and 3 dpi and n=4 animals thereafter.

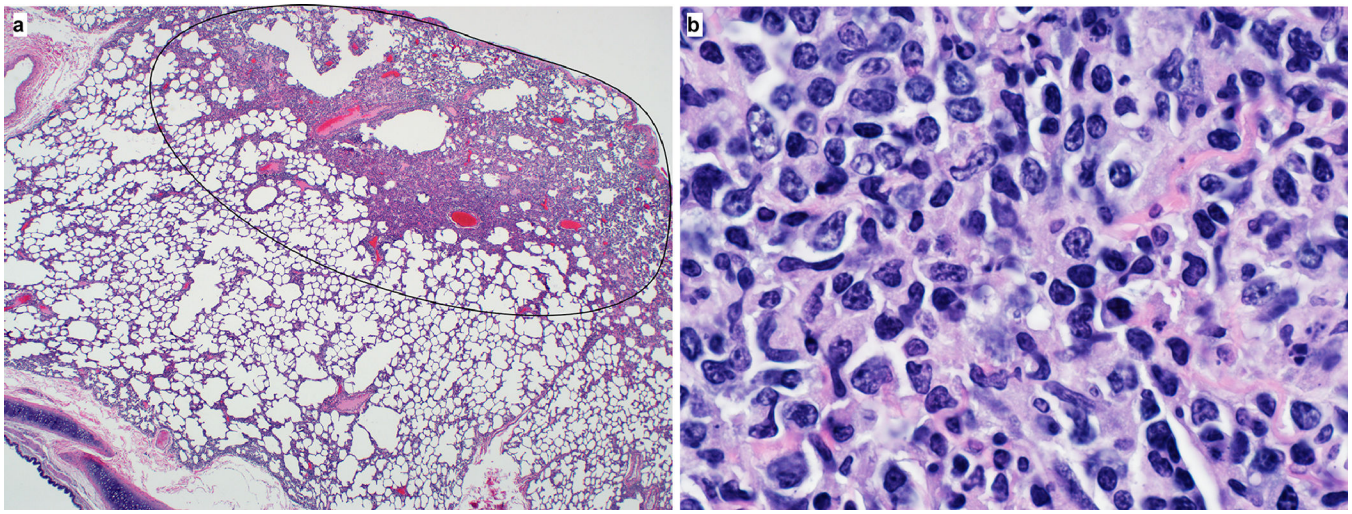

Extended Data Figure 4. Histological lesions in lungs of a rhesus macaque infected with SARS-CoV-2.

(a) This low magnification figure displays the focal nature of SARS-CoV-2 lesions in the lungs of animals euthanized on 3 dpi. The circle indicates the lung affected by lesion; the

Author Manuscript Author Manuscript Author Manuscript Author Manuscript

remaining lung tissue is healthy. (b) Lymphocytes surround pulmonary vessels. Magnification 500x. Tissue sections were collected from the same anatomical location for each animal; three tissue sections were prepared from each of the 6 lung lobes. In total, 18 lung sections were evaluated for each animal (n=4); representative images are displayed.

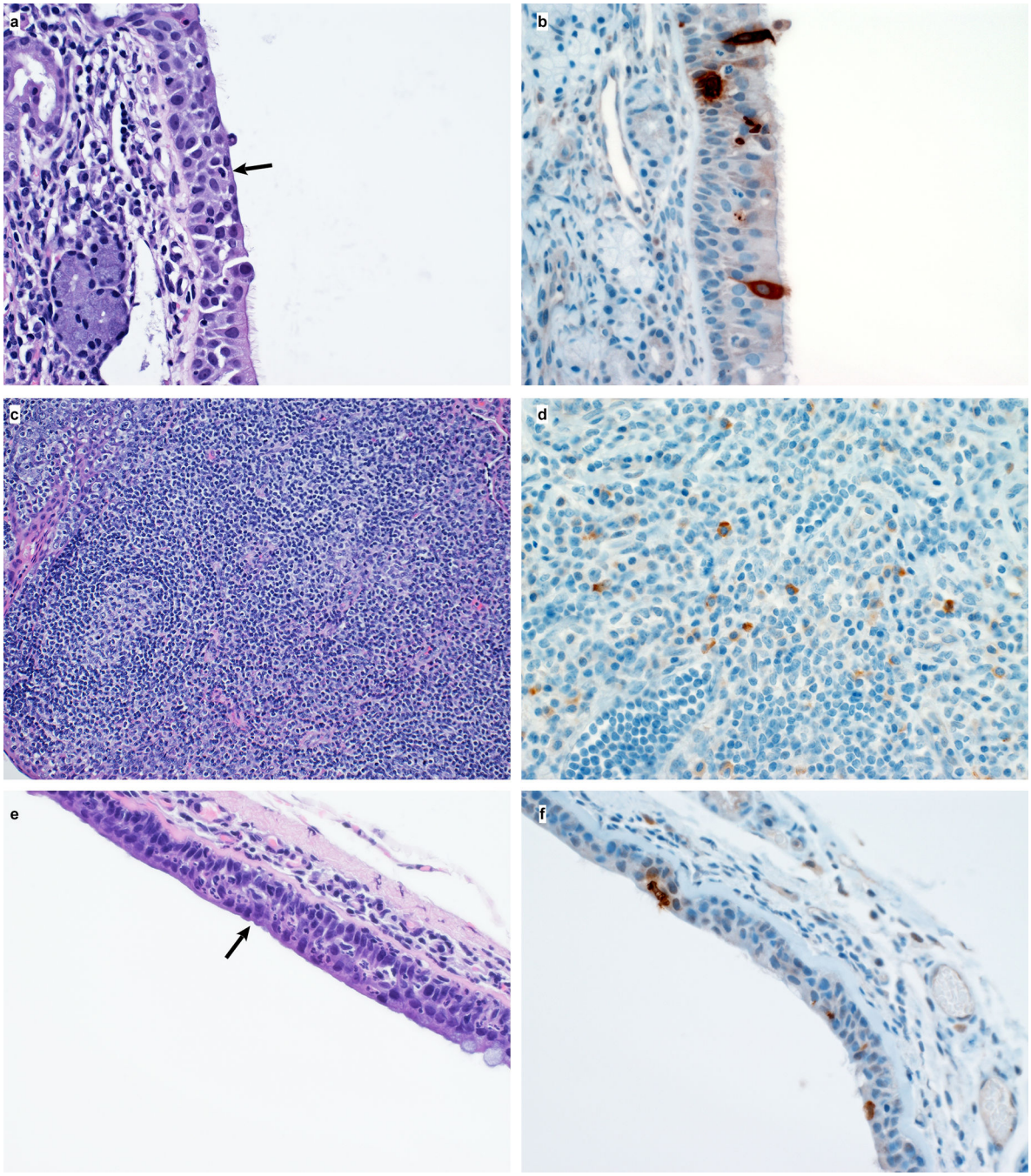

Extended Data Figure 5. Histological changes in the respiratory tract of rhesus macaques infected with SARS-CoV-2.

(a) Squamous metaplasia of nasal turbinate respiratory epithelium (arrow). Magnification 400x. (b) SARS-CoV-2 antigen is detected by immunohistochemistry in respiratory

Author Manuscript Author Manuscript Author Manuscript Author Manuscript

epithelium of the nasal turbinate. Magnification 400x. (c) Essentially normal tonsil. Magnification 400x. (d) SARS-CoV-2 antigen is detected by immunohistochemistry in tonsillar macrophages. Magnification 400x. (e) Squamous metaplasia of tracheal columnar epithelium (arrow). Magnification 400x. (f) SARS-CoV-2 antigen is detected by immunohistochemistry in tracheal columnar epithelium. Magnification 400x. Tissue sections were collected from the same anatomical location for each animal (n=4) and organ; one tissue section was evaluated of the nasal turbinates of each animal; three tissue sections were evaluated from tonsil and trachea.

Author Manuscript Author Manuscript Author Manuscript Author Manuscript

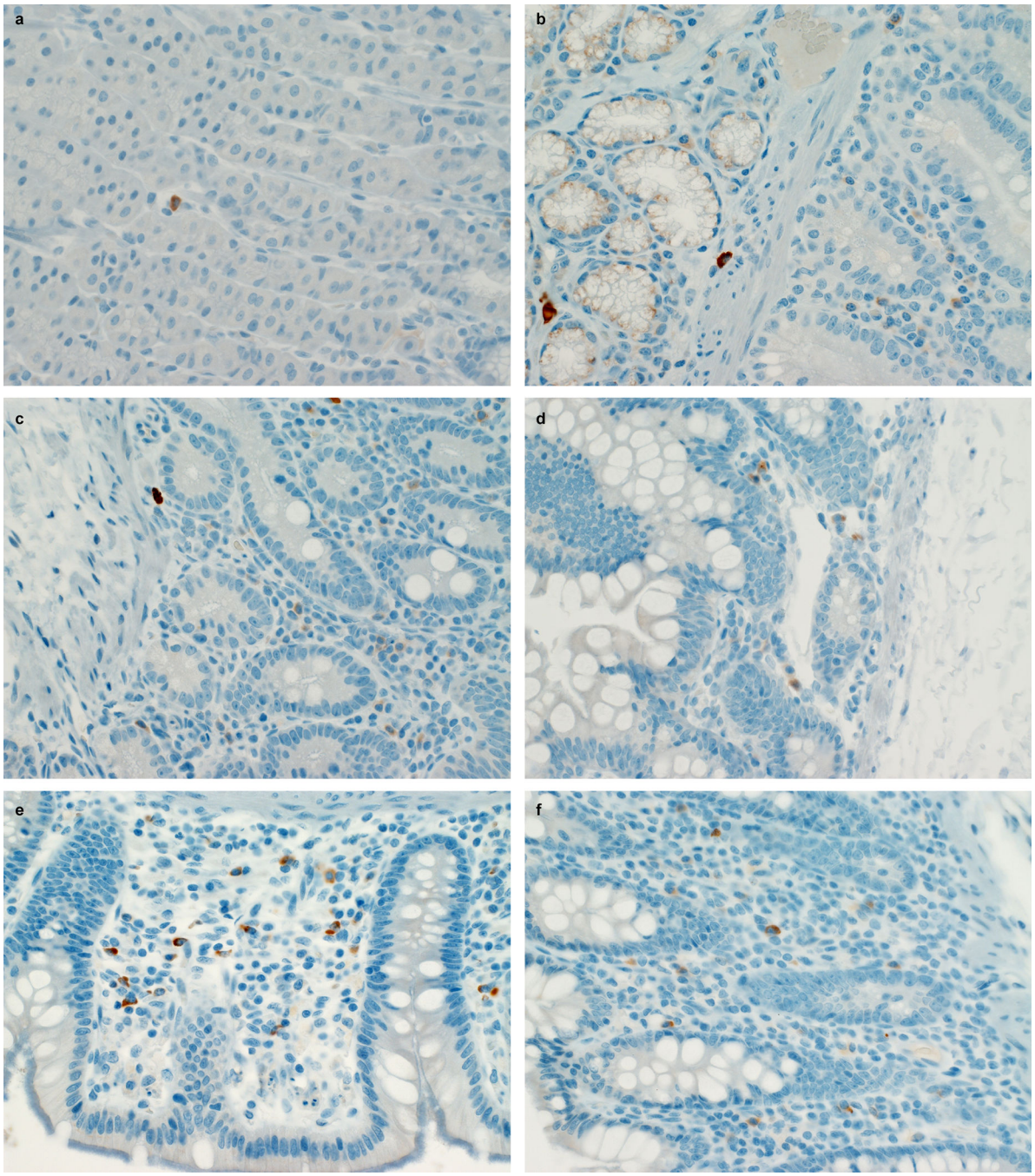

Extended Data Figure 6. SARS-CoV-2 antigen in the gastrointestinal tract of a rhesus macaque infected with SARS-CoV-2.

Mononuclear cells staining positive for SARS-CoV-2 antigen in the lamina propria of stomach (a), duodenum (b), jejunum (c), ileum (d), cecum (e) and colon (f) of an animal infected with SARS-CoV-2 and euthanized on 3 dpi. Tissue sections were collected from the same anatomical location for each animal (n=4) and organ; three tissue sections were evaluated from each animal and organ.

Author Manuscript Author Manuscript Author Manuscript Author Manuscript

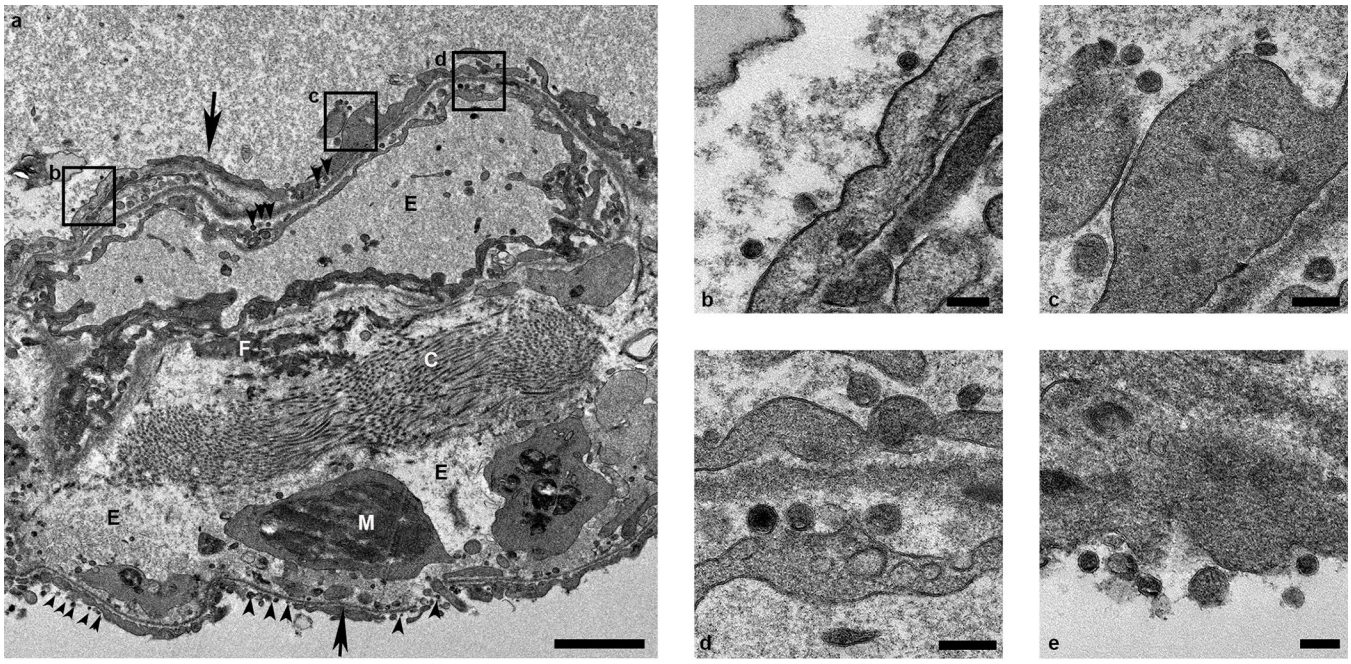

Extended Data Figure 7. Ultrastructural analysis of lungs of rhesus macaques infected with SARS-CoV-2.

Lung tissue collected on 3 dpi was analyzed by transmission electron microscopy. The alveolar interstitium is expanded by edema (E), fibrin (F) and mononuclear (M) inflammatory cells (a). Normal collagen fibers (c) and multiple virions (arrowheads) line type I pneumocytes (arrows). Boxes in (a) indicate areas enlarged in (b-d). Scale bar in (a) represents 2μm, scale bars in (b-e) represent 0.2 μm. Three tissue samples were collected from each animal (n=4) and cut into 6 samples for analysis; a minimum of 2 samples were analyzed per animal (n=4).

Author Manuscript Author Manuscript Author Manuscript Author Manuscript

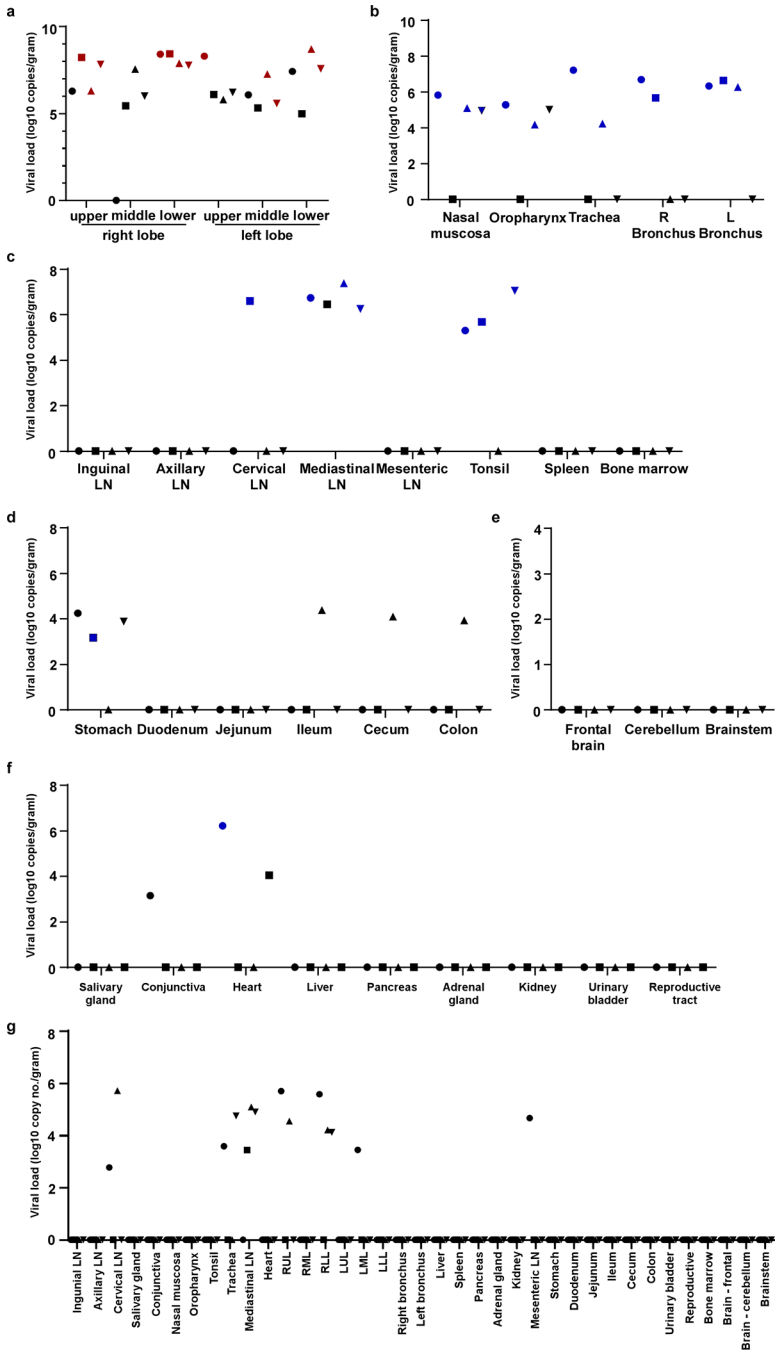

Extended Data Figure 8. Viral loads in tissues collected from rhesus macaques infected with SARS-CoV-2.

Eight adult rhesus macaques were inoculated with SARS-CoV-2 isolate nCoV-WA1–2020 and euthanized on 3 (n=4) and 21 (n=4) dpi. Thirty-seven tissues were collected at necropsy and analyzed for the presence of viral RNA by qRT-PCR. Tissues are grouped by lung lobes collected on 3 dpi (a), with red symbols indicating tissues from which virus could be isolated in Vero E6 cells; other tissues from the respiratory tract on 3dpi (b); lymphoid tissues on 3 dpi (c); gastrointestinal tissueson 3 dpi (d); the central nervous system on 3 dpi (e); remaining tissues on 3 dpi (f); and all tissues collected on 21 dpi (g). Blue symbols in b-

Author Manuscript Author Manuscript Author Manuscript Author Manuscript

g indicate that viral mRNA was also detected in these tissues. Identical symbols have been used to denote identical animals throughout the figures in this manuscript. LN: lymph node; RUL: right upper lung lobe; RML: right middle lung lobe; RLL: right lower lung lobe; LUL: left upper lung lobe; LML: left middle lung lobe; LLL: left lower lung lobe; R: right; L: left.

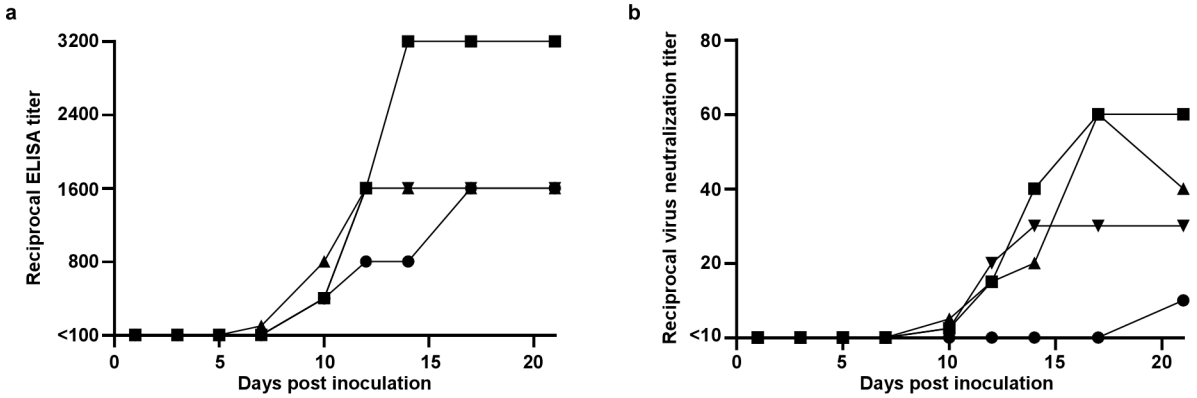

Extended Data Figure 9. Antibody response in rhesus macaques infected with SARS-CoV-2.
Sera collected after inoculation were tested for the presence of IgG against SARS-CoV-2 spike in ELISA (a) and for the presence of neutralizing antibodies in a microneutralization assay (b). All sera were analyzed in duplicate. Identical symbols have been used to denote identical animals throughout the figures in this manuscript.

Extended Data Table 1.

Clinical signs observed in rhesus macaques inoculated with SARS-CoV-2.

Animal	Clinical signs observed 1–6 dpi	Clinical signs observed 7–21 dpi	Observations at necropsy*
RM1	Hunched posture; piloerection; tachypnea; flushed appearance; red eyes; very agitated; reduced appetite; mildly dehydrated. Euthanized 3 dpi.	N/A	Gross lung lesions. Enlarged tonsils and mediastinal lymph nodes. Fluid-filled stomach, small and large intestine.
RM2	Piloerection; dyspnea; reduced appetite. Euthanized 3 dpi.	N/A	Fluid-filled stomach, small and large intestine.
RM3	Piloerection; tachypnea; flushed appearance; reduced appetite; mildly dehydrated. Euthanized 3 dpi.	N/A	Epistaxis. Gross lung lesions. Enlarged mediastinal lymph nodes. Fluid-filled stomach, small and large intestine.
RM4	Hunched posture; piloerection; tachypnea; dyspnea; reduced appetite. Euthanized 3 dpi.	N/A	Gross lung lesions. Foamy exudate from trachea. Enlarged mediastinal lymph nodes. Fluid-filled stomach, small and large intestine.
RM5	Hunched posture; piloerection; tachypnea; dyspnea; reduced appetite.	Tachypnea; dyspnea; reduced appetite; mildly dehydrated. Recovered on 9 dpi.	Gross lung lesions. Enlarged mesenteric lymph nodes.
RM6	Hunched posture; piloerection; tachypnea; dyspnea; reduced appetite; serous nasal discharge.	Piloerection; bradypnea; mildly dehydrated; crusty nasal discharge. Recovered on 10 dpi.	None.

Author Manuscript Author Manuscript Author Manuscript Author Manuscript

Animal	Clinical signs observed 1–6 dpi	Clinical signs observed 7–21 dpi	Observations at necropsy*
RM7	Hunched posture; piloerection; pale appearance; tachypnea; dyspnea; irregular; labored respirations; anorexia; mildly dehydrated; serous nasal discharge.	Hunched posture; piloerection; pale appearance; tachypnea; dyspnea; reduced appetite; mildly dehydrated; crusty nasal discharge. Recovered on 17 dpi.	None.
RM8	Hunched posture; piloerection; pale appearance; increased, dyspnea; reduced appetite; serous nasal discharge.	Hunched posture; piloerection; pale appearance; increased, dyspnea; nasal discharge; reduced appetite; mildly dehydrated; serous nasal discharge. Recovered on 13 dpi.	Gross lung lesions.

* Incidental observations not related to coronavirus infection were omitted from this table.

Supplementary Material

Refer to Web version on PubMed Central for supplementary material.

Acknowledgements

The authors would like to thank Susan Gerber and Natalie Thornburg (CDC) for providing the SARS-CoV-2 isolate used in this study; Barney Graham, Kizzmekia Corbett and Olubukola Abiona at the Vaccine Research Center (NIAID, NIH) for providing spike protein for serology; Anita Mora (NIAID, NIH) for help with figure design and staff of the Rocky Mountain Veterinary Branch (NIAID, NIH) for animal care. This study was supported by the Intramural Research Program, NIAID, NIH.

References

1. Wu F et al. A new coronavirus associated with human respiratory disease in China. Nature, doi:10.1038/s41586-020-2008-3 (2020).
2. Zhu N et al. A Novel Coronavirus from Patients with Pneumonia in China, 2019. N Engl J Med 382, 727–733, doi:10.1056/NEJMoa2001017 (2020). [PubMed: 31978945]
3. Organization, W. H. Coronavirus disease (COVID-2019) situation reports, <https://www.who.int/emergencies/diseases/novel-coronavirus-2019/situation-reports/> (2020).
4. Yang W et al. Clinical characteristics and imaging manifestations of the 2019 novel coronavirus disease (COVID-19):A multi-center study in Wenzhou city, Zhejiang, China. J Infect, doi:10.1016/j.jinf.2020.02.016 (2020).
5. Yang X et al. Clinical course and outcomes of critically ill patients with SARS-CoV-2 pneumonia in Wuhan, China: a single-centered, retrospective, observational study. Lancet Respir Med, doi:10.1016/S2213-2600(20)30079-5 (2020).
6. Silverstein WK, Stroud L, Cleghorn GE & Leis JA First imported case of 2019 novel coronavirus in Canada, presenting as mild pneumonia. Lancet 395, 734, doi:10.1016/S0140-6736(20)30370-6 (2020). [PubMed: 32061312]
7. Arentz M et al. Characteristics and Outcomes of 21 Critically Ill Patients With COVID-19 in Washington State. JAMA, doi:10.1001/jama.2020.4326 (2020).
8. Zhou F et al. Clinical course and risk factors for mortality of adult inpatients with COVID-19 in Wuhan, China: a retrospective cohort study. Lancet, doi:10.1016/S0140-6736(20)30566-3 (2020).
9. Guan WJ et al. Clinical Characteristics of Coronavirus Disease 2019 in China. N Engl J Med, doi:10.1056/NEJMoa2002032 (2020).
10. Shi H et al. Radiological findings from 81 patients with COVID-19 pneumonia in Wuhan, China: a descriptive study. Lancet Infect Dis, doi:10.1016/S1473-3099(20)30086-4 (2020).
11. Zou L et al. SARS-CoV-2 Viral Load in Upper Respiratory Specimens of Infected Patients. N Engl J Med, doi:10.1056/NEJMc2001737 (2020).

Author Manuscript Author Manuscript Author Manuscript Author Manuscript

12. Kim JY et al. Viral Load Kinetics of SARS-CoV-2 Infection in First Two Patients in Korea. J Korean Med Sci 35, e86, doi:10.3346/jkms.2020.35.e86 (2020). [PubMed: 32080991]
13. Tang A et al. Detection of Novel Coronavirus by RT-PCR in Stool Specimen from Asymptomatic Child, China. Emerg Infect Dis 26, doi:10.3201/eid2606.200301 (2020).
14. Harcourt J et al. Severe Acute Respiratory Syndrome Coronavirus 2 from Patient with 2019 Novel Coronavirus Disease, United States. Emerg Infect Dis 26, doi:10.3201/eid2606.200516 (2020).
15. Everds NE et al. Interpreting stress responses during routine toxicity studies: a review of the biology, impact, and assessment. Toxicol Pathol 41, 560–614, doi:10.1177/0192623312466452 (2013). [PubMed: 23475558]
16. Wang D et al. Clinical Characteristics of 138 Hospitalized Patients With 2019 Novel Coronavirus-Infected Pneumonia in Wuhan, China. JAMA, doi:10.1001/jama.2020.1585 (2020).
17. Assiri A et al. Epidemiological, demographic, and clinical characteristics of 47 cases of Middle East respiratory syndrome coronavirus disease from Saudi Arabia: a descriptive study. Lancet Infect Dis 13, 752–761, doi:10.1016/S1473-3099(13)70204-4 (2013). [PubMed: 23891402]
18. Booth CM et al. Clinical features and short-term outcomes of 144 patients with SARS in the greater Toronto area. JAMA 289, 2801–2809, doi:10.1001/jama.289.21.JOC30885 (2003). [PubMed: 12734147]
19. Lan L et al. Positive RT-PCR Test Results in Patients Recovered From COVID-19. JAMA, doi:10.1001/jama.2020.2783 (2020).
20. Tian S et al. Pulmonary Pathology of Early-Phase 2019 Novel Coronavirus (COVID-19) Pneumonia in Two Patients With Lung Cancer. J Thorac Oncol, doi:10.1016/j.jtho.2020.02.010 (2020).
21. Xu Z et al. Pathological findings of COVID-19 associated with acute respiratory distress syndrome. Lancet Respir Med, doi:10.1016/S2213-2600(20)30076-X (2020).
22. Ng DL et al. Clinicopathologic, Immunohistochemical, and Ultrastructural Findings of a Fatal Case of Middle East Respiratory Syndrome Coronavirus Infection in the United Arab Emirates, April 2014. Am J Pathol 186, 652–658, doi:10.1016/j.ajpath.2015.10.024 (2016). [PubMed: 26857507]
23. Nicholls JM et al. Lung pathology of fatal severe acute respiratory syndrome. Lancet 361, 1773–1778, doi:10.1016/s0140-6736(03)13413-7 (2003). [PubMed: 12781536]
24. Ding Y et al. The clinical pathology of severe acute respiratory syndrome (SARS): a report from China. J Pathol 200, 282–289, doi:10.1002/path.1440 (2003). [PubMed: 12845623]
25. Roman Wölfel* Victor M Corman WG, Seilmaier Michael, Zange Sabine, Müller Marcel A., Niemeyer Daniela, Jones Kelly Terence C., Vollmar Patrick, Rothe Camilla, Hoelscher Michael, Bleicker Tobias, Brünink Sebastian, Schneider Julia, Ehmann Rosina, Zwirglmaier Katrin, Drosten Christian, Wendtner Clemens. Virological assessment of hospitalized cases of coronavirus disease 2019. MEDRXIV (2020).
26. Zhao Y, Wang Liu, Liao Su, Wang Yuan, Li Li, Qian Hong, Wang Liu, Wang He, Li He, Zhang Ge, Liu Zhang, Xia Zhang. Antibody responses to SARS-CoV-2 in patients of novel coronavirus disease 2019. medRxiv (2020).

References

27. Haley PJ, Muggenburg BA, Rebar AH, Shopp GM & Bice DE Bronchoalveolar lavage cytology in cynomolgus monkeys and identification of cytologic alterations following sequential saline lavage. Vet Pathol 26, 265–273, doi:10.1177/030098588902600312 (1989). [PubMed: 2763415]
28. Krombach F et al. Short-term and long-term effects of serial bronchoalveolar lavages in a nonhuman primate model. Am J Respir Crit Care Med 150, 153–158, doi:10.1164/ajrccm.150.1.8025742 (1994). [PubMed: 8025742]
29. Corman VM et al. Detection of 2019 novel coronavirus (2019-nCoV) by real-time RT-PCR. Euro Surveill 25, doi:10.2807/1560-7917.ES.2020.25.3.2000045 (2020).
30. van Doremalen N et al. High Prevalence of Middle East Respiratory Coronavirus in Young Dromedary Camels in Jordan. Vector Borne Zoonotic Dis 17, 155–159, doi:10.1089/vbz.2016.2062 (2017). [PubMed: 28009529]

Author Manuscript Author Manuscript Author Manuscript Author Manuscript

31. Wrapp D et al. Cryo-EM structure of the 2019-nCoV spike in the prefusion conformation. Science 367, 1260–1263, doi:10.1126/science.abb2507 (2020). [PubMed: 32075877]

Author Manuscript Author Manuscript Author Manuscript Author Manuscript

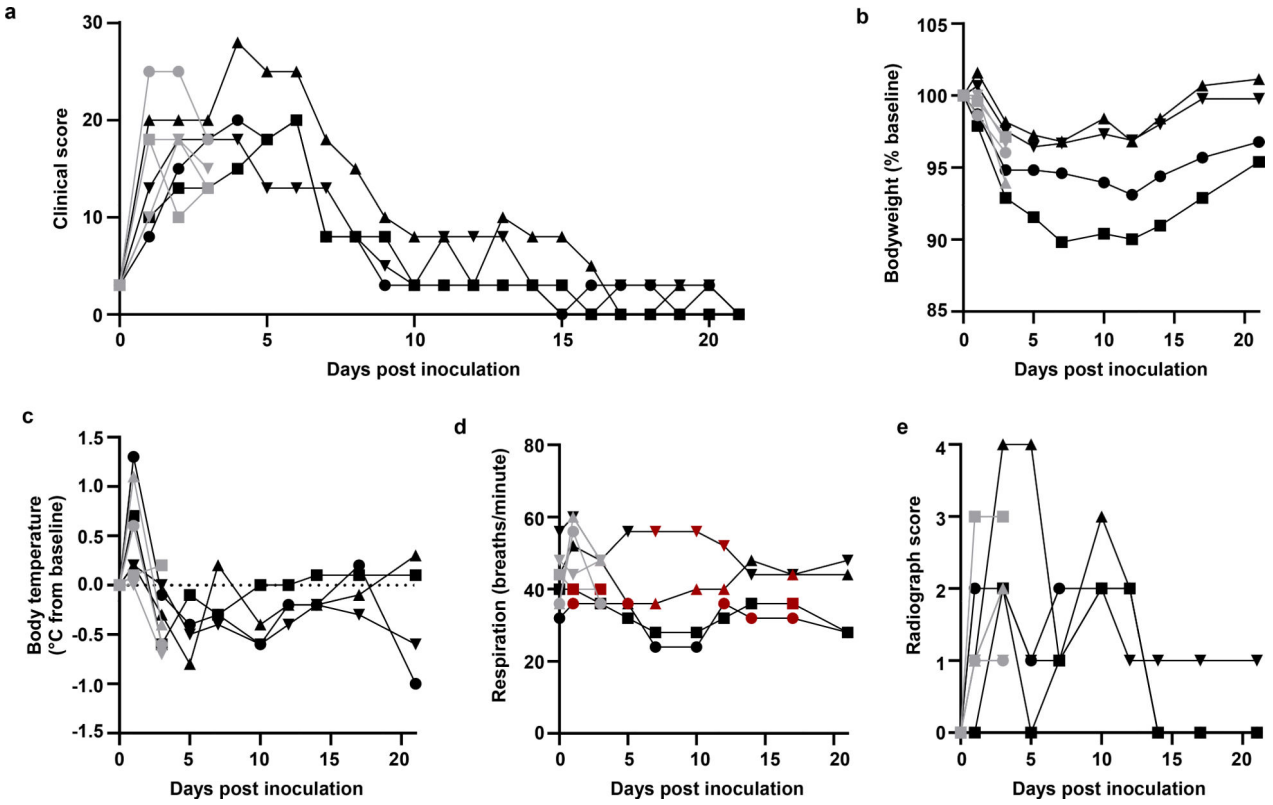

Figure 1. Rhesus macaques infected with SARS-CoV-2 develop respiratory disease.

After inoculation with SARS-CoV-2, animals were observed for disease signs and scored according to a pre-established clinical scoring sheet (a). On clinical exams, body weight (b), and body temperature (c) were measured. Respiration rate was measured, and breathing pattern was recorded, with irregular respiration patterns indicated in red (d). Ventro-dorsal and lateral radiographs were taken on clinical exam days and scored for the presence of pulmonary infiltrates (0: normal; 1: mild interstitial pulmonary infiltrates; 2: moderate pulmonary infiltrates perhaps with partial cardiac border effacement and small areas of pulmonary consolidation; 3: severe interstitial infiltrates, large areas of pulmonary consolidation, alveolar patterns and air bronchograms). Individual lobes were scored and scores per animal per day totaled (e). Grey: animals euthanized 3 dpi; black: animals euthanized 21 dpi. Identical symbols have been used to denote identical animals throughout this manuscript.

Author Manuscript Author Manuscript Author Manuscript Author Manuscript

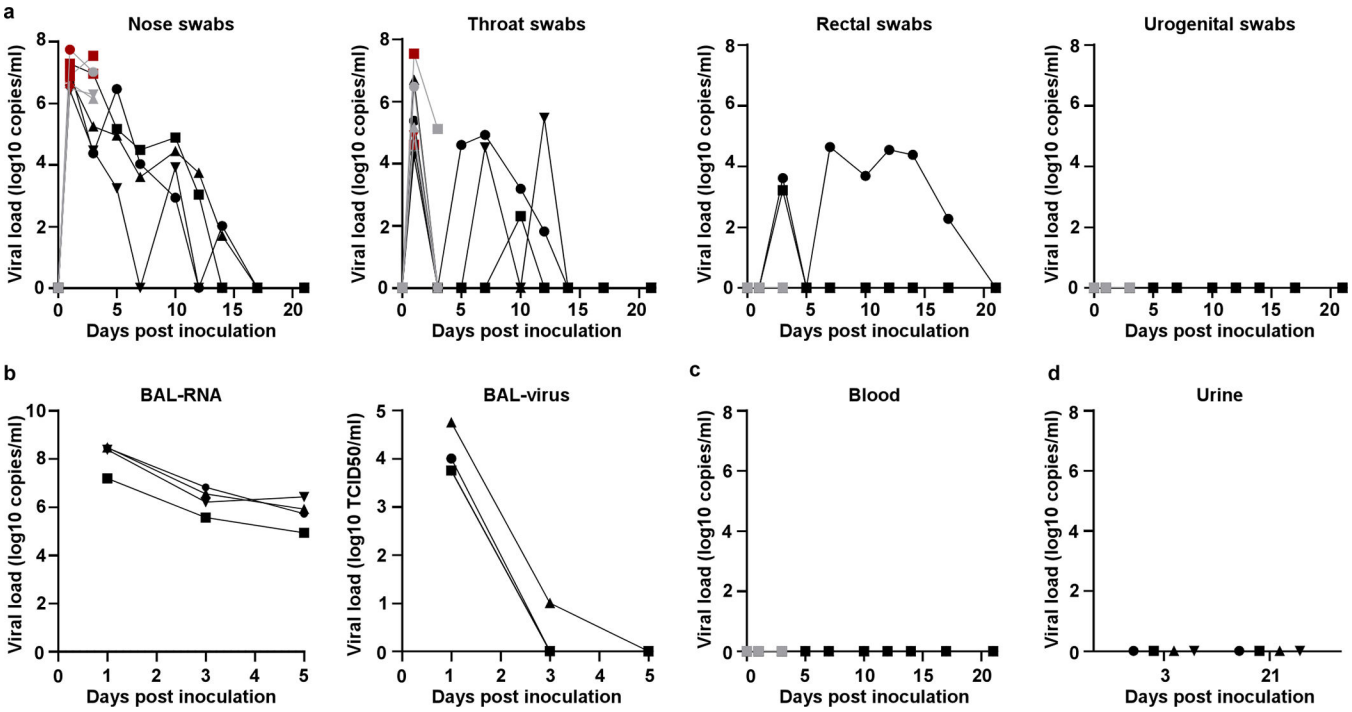

Figure 2. Viral loads in respiratory samples and bodily fluids.

After inoculation, nose, throat, rectal and urogenital swabs were collected; viral loads in these samples were determined by qRT-PCR (a). On 1, 3, and 5 dpi, bronchoalveolar lavages were performed on the 4 animals remaining in the study through 21 dpi; viral loads and virus titers were determined in these samples. Viral loads were determined in blood collected during clinical exams (c) and urine collected at necropsy on 3 and 21 (d). Grey: animals euthanized 3 dpi; black: animals euthanized 21 dpi; red: virus was isolated from these samples. Identical symbols have been used to denote identical animals this manuscript.

Author Manuscript Author Manuscript Author Manuscript Author Manuscript

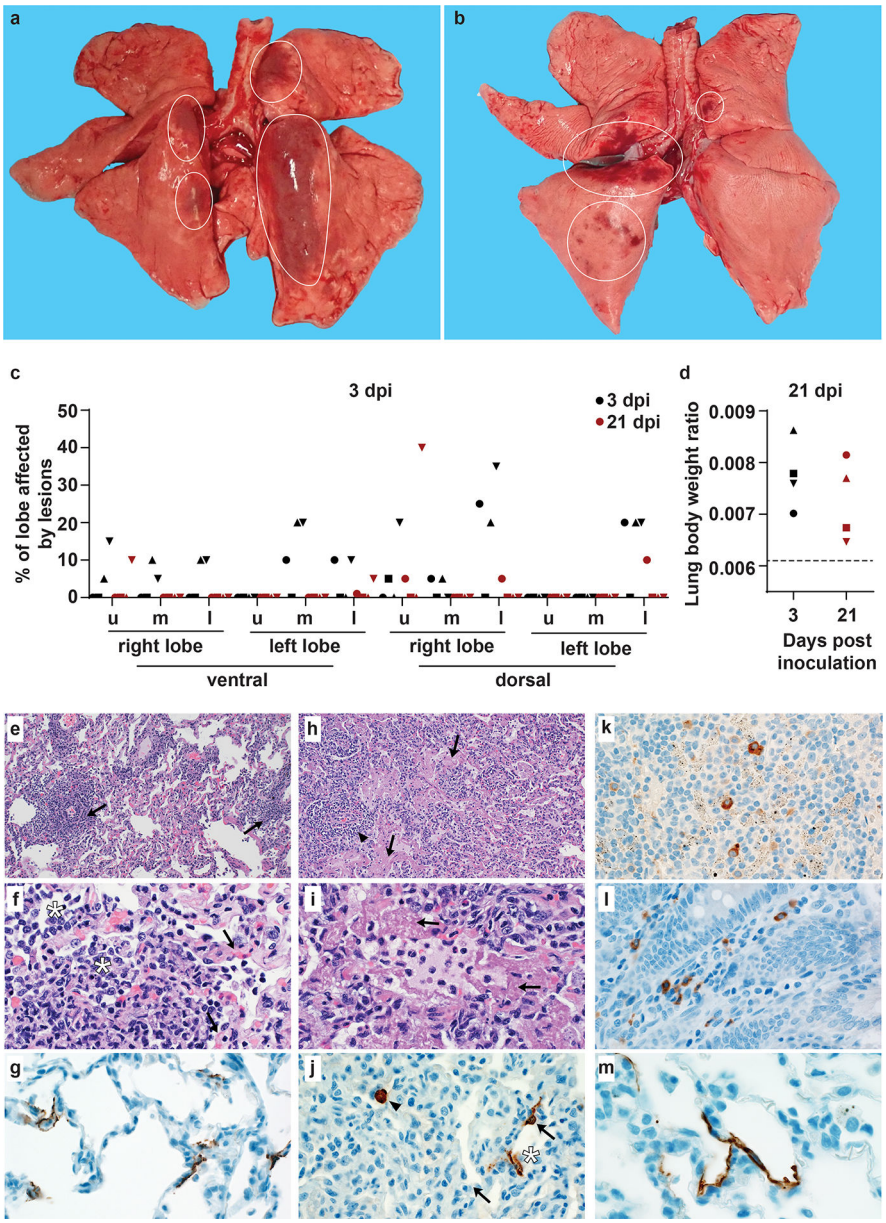

Figure 3. Pathological changes in rhesus macaques infected with SARS-CoV-2.

Four rhesus macaques were euthanized on 3 and 21 dpi. Grossly, lungs showed focal areas of hilar consolidation and hyperemia (circles) on 3 dpi (a) and multifocal, random consolidation and hyperemia (circles) on 21 dpi (b). The percentage of the area of the lungs affected by gross lesions was estimated (c), and lung weight to bodyweight ratio was calculated. (d). The dotted line represents baseline ratio calculated from an in-house collection of rhesus macaque lung and bodyweights from animals with grossly normal lungs. Histological analysis was performed on tissues collected at 3 dpi (e-i). Tissue sections were collected from the same anatomical location for each animal; three tissue sections were prepared from each of the 6 lung lobes. In total, 18 lung sections were evaluated for each animal; representative images are displayed. (e) Pulmonary vessels surrounded by moderate numbers of lymphocytes and fewer macrophages (arrows). (f) Alveoli filled with small to

Author Manuscript Author Manuscript Author Manuscript Author Manuscript

moderate numbers of macrophages and neutrophils (asterisks). Adjacent alveolar interstitium (arrows) is thickened by edema, fibrin, neutrophils, lymphocytes and macrophages. (g) SARS-CoV-2 antigen detected by immunohistochemistry in type I pneumocytes. (h) Pulmonary vessels bounded by lymphocytes (arrowhead) and hyaline membranes (arrows) line alveolar spaces. (i) Hyaline membranes line alveoli (arrows). (j) SARS-CoV-2 antigen detected by immunohistochemistry in type I pneumocytes (asterisk) and type II pneumocytes (arrow) as well as alveolar macrophages (arrowheads). (k) SARS-CoV-2 antigen detected by immunohistochemistry in macrophages in a mediastinal lymph node. (l) SARS-CoV-2 antigen detected by immunohistochemistry in macrophages and lymphocytes in the lamina propria of the cecum. (m) SARS-CoV-2 detected by immunohistochemistry in type I pneumocytes. Magnification: e, h 100x; f, g, I, j, k, l 400x; m: 1000x. u: upper; m: middle; l: lower